detritus | Multidisciplinary Journal for Circular Economy and Sustainable Management of Residues

CISA

RECYCLING-ORIENTED IDENTIFICATION OF FOSSIL-BASED PLASTICS AND BIOPLASTICS IN PACKAGING WASTE USING HYPERSPECTRAL IMAGING AND HIERARCHICAL CLASSIFICATION

Giuseppe Bonifazi, Giuseppe Capobianco, Paola Cucuzza * and Silvia Serranti

Department of Chemical Engineering, Materials & Environment, Sapienza University of Rome, Via Eudossiana, 18, 00184 Rome, Italy

Article Info:
Received:
23 June 2026
Revised:
4 September 2026
Accepted:
9 September 2026
Available online:
20 September 2026

Keywords:
Hyperspectral imaging
Bioplastics identification
Machine learning
Plastic waste recycling

ABSTRACT

The increasing use of bioplastics in packaging leads to their presence within conventional plastic waste streams, where even minor cross-contamination can compromise recycled material quality. Therefore, rapid and efficient material identification strategies are required to support high-purity sorting processes. This study evaluates the applicability of short-wave infrared hyperspectral imaging (SWIR-HSI: 1000-2500 nm) combined with chemometric and machine-learning approaches for the automatic classification of fossil-based plastic and bioplastic flakes from household packaging waste. Five fossil-based polymers commonly used for plastic packaging, i.e., polyethylene terephthalate (PET), high-density polyethylene (HDPE), polypropylene (PP), polystyrene (PS), expanded polystyrene (EPS), and three polylactic acid (PLA)-based bioplastics derived from disposable food packaging items were investigated. Hyperspectral images of the studied samples were acquired in the SWIR range and divided into calibration and validation datasets to develop and evaluate the proposed classification model. After spectral preprocessing, Principal Component Analysis (PCA) was used to explore class separability and guide the development of a hierarchical Partial Least Squares-Discriminant Analysis (Hi-PLS-DA) model. The proposed methodology achieved high predictive performance on the independent validation dataset, with sensitivity and specificity ranging from 0.96 to 1.00. Although conceived as a proof of concept, the proposed approach demonstrates the feasibility of combining SWIR-HSI with hierarchical chemometric classification for recycling-oriented identification of fossil-based plastics and PLA-based bioplastics, supporting the development of more effective sensor-based sorting strategies.

1. INTRODUCTION

The global increase in plastic production is associated with a substantial growth in plastic waste generation, with mismanaged plastic waste projected to nearly double by 2050 if current management practices remain unchanged (Pottinger et al., 2024). Alongside conventional fossil-based polymers, the packaging sector is progressively introducing bioplastics, often perceived as environmentally friendly alternatives, particularly for packaging materials and disposable items, in line with the European Packaging and Packaging Waste Regulation (PPWR) (European Commission, 2024). However, despite their growing adoption and potential as sustainable alternatives to traditional plastics, their actual environmental benefits and end-of-life management remain widely debated in the scientific literature (Lavagnolo et al., 2020; Cucina et al., 2021; Das et al., 2025). Furthermore, although recent European regulations promote the use of compostable packaging for selected applications (European Bioplastics, 2025), the increasing diffusion of bioplastics raises additional challenges for waste management systems, particularly when these materials enter conventional plastic recycling streams, as even small contamination levels can compromise the quality of recycled materials (Alaerts et al., 2018). Materials Recovery Facilities (MRFs) therefore face increasing operational challenges. Traditional sorting strategies rely on the recognition of established polymer families, whereas the integration of bioplastics requires the introduction of additional material classes and updated decision logics to ensure reliable material recovery (Gadaleta et al., 2023). The introduction of bioplastics into existing municipal solid waste management systems may affect treatment efficiency, requiring appropriate sorting strategies (De Gisi et al., 2022). In practice, bioplastics that are intended to

* Corresponding author:
Paola Cucuzza
email: paola.cucuzza@uniroma1.it

Detritus / In press / pages 1-9
https://doi.org/10.31025/2611-4135/2026.20615

be collected with organic waste are frequently mis-sorted and may enter conventional plastic recycling streams (De Gisi et al., 2022). For this reason, their identification during sorting becomes important to prevent contamination and support appropriate waste management (Ulrici et al., 2013; McLauchlin et al., 2014; Cosate de Andrade et al., 2016; Alaerts et al., 2018). In this context, sensor-based sorting represents a key strategy to improve the quality of recovered plastic fractions, as it enables rapid, non-destructive and automated material identification directly along sorting lines. However, the increasing heterogeneity of post-consumer packaging waste makes material recognition more challenging. Spectral variability may arise from polymer formulation, color, thickness, surface roughness, additives, fillers, ageing, contamination and object geometry (Araujo-Andrade et al., 2021).

Among sensor-based sorting technologies, near infrared (NIR) and short-wave infrared (SWIR) optical detection is widely used for polymer recognition in recycling applications, while hyperspectral imaging (HSI) represents an advanced approach because it enables pixel-wise chemical characterization by simultaneously acquiring spatial and spectral information (Serranti et al., 2020; Araujo-Andrade et al., 2021; Bonifazi et al., 2025a). These sensor-based approaches enable rapid and non-destructive material characterization, supporting automated sorting operations in modern recycling facilities. Nevertheless, the high dimensionality of hyperspectral data and the spectral similarity among plastic materials require robust chemometric and machine-learning approaches to transform spectral signatures into reliable classification rules, as demonstrated in similar case studies (Tamin et al., 2021; Henriksen et al., 2022; Bonifazi et al., 2022, 2025b; Cheng et al., 2025; Li et al., 2025; Serranti et al., 2026). On this basis, the present work evaluates the applicability of SWIR-HSI (1000-2500 nm) combined with PCA-guided hierarchical classification strategy for the recycling-oriented identification of fossil-based plastics and PLA-based bioplastics in packaging waste flakes.

2. MATERIALS AND METHODS

2.1 Fossil-based plastic and PLA-based bioplastic samples

The investigated dataset consisted of plastic packaging waste flakes (approximately 1–5 cm in size) obtained by mechanical comminution of post-consumer household plastic packaging items commonly found in municipal waste streams. The samples exhibit a wide range of colors, including both transparent and opaque plastic materials (Figure 1). The total number of studied samples was 240 flakes, divided into:

- 150 flakes of fossil-based plastics from packaging, comprising 30 flakes of expanded polystyrene (EPS) sourced from food packaging, 30 flakes of polystyrene (PS) derived from yogurt cups, 30 flakes of polyethylene terephthalate (PET) sourced from water bottles, 30 flakes of high-density polyethylene (HDPE) from detergent bottles and food containers, and 30 flakes of polypropylene (PP) collected from rigid food containers.
- 90 flakes derived from three types of polylactic acid (PLA)-based bioplastic packaging items. These consisted of 30 flakes obtained from the comminution of PLA-based drinking cups (labeled as CUP), 30 flakes from PLA-based coffee capsules (labeled as CAPSULE), and 30 flakes from PLA-based disposable plates (labeled as PLATE).

Figure 1a shows the samples used as calibration dataset, whereas Figure 1b shows the samples used as validation dataset.

2.2 Hyperspectral imaging acquisition

Hyperspectral images were acquired at the Raw Materials Laboratory (RawMaLab) of the Department of Chemical Engineering, Materials & Environment, Sapienza University of Rome, using the pushbroom Sisuchema XL™ Workstation equipped with the ImSpector™ N25E spectrograph (Specim, Spectral Imaging Ltd., Oulu, Finland). The imaging configuration consisted of a 15 mm lens providing a field of view of approximately 20 cm and a pixel resolution of 625 μm/pixel. The lighting was reproduced by applying a diffuse line illumination unit. The acquired hyperspectral images were automatically calibrated in reflectance using an internal reference standard before line-by-line scanning.

2.3 Data processing and performance evaluation

PLS_Toolbox (version 9.3, Eigenvector Research Inc.) operating in the MATLAB® environment (version R2024b, The MathWorks Inc.) was used for spectral preprocessing, exploratory analysis and classification modelling. Different pre-processing techniques and combinations of algorithms were tested to enhance relevant spectral information and reduce unwanted spectral variability, following the examples usually adopted in literature (Rinnan et al., 2009; Vidal and Amigo, 2012). Standard normal variate (SNV) was applied to reduce multiplicative scattering effects related to differences in particle geometry, surface roughness and illumination conditions (Eigenvector Research, 2021). Subsequently, a first derivative using the Savitzky–Golay method was applied to enhance spectral band resolution and reduce baseline-related effects, thereby reducing noise amplification (Eigenvector Research, 2019). In addition, the Gap Segment first derivative was evaluated as an alternative derivative algorithm. This method estimates the first derivative using spectral segments separated by a defined gap, reducing the influence of high-frequency noise while enhancing relevant spectral features (Eigenvector Research, 2013). Finally, mean centering was performed to center the variables, facilitating multivariate modeling by placing all variables on a common scale around zero (Eigenvector Research, 2011).

Principal component analysis (PCA) was chosen to perform exploratory analysis of class variability, to identify and remove outliers (Bro and Smilde, 2014).

Based on PCA insights, a hierarchical classification model strategy was developed to identify the eight target spectral classes: EPS, PS, PET, HDPE, PP, CUP, CAPSULE, and PLATE. A hierarchical classification approach is suit-

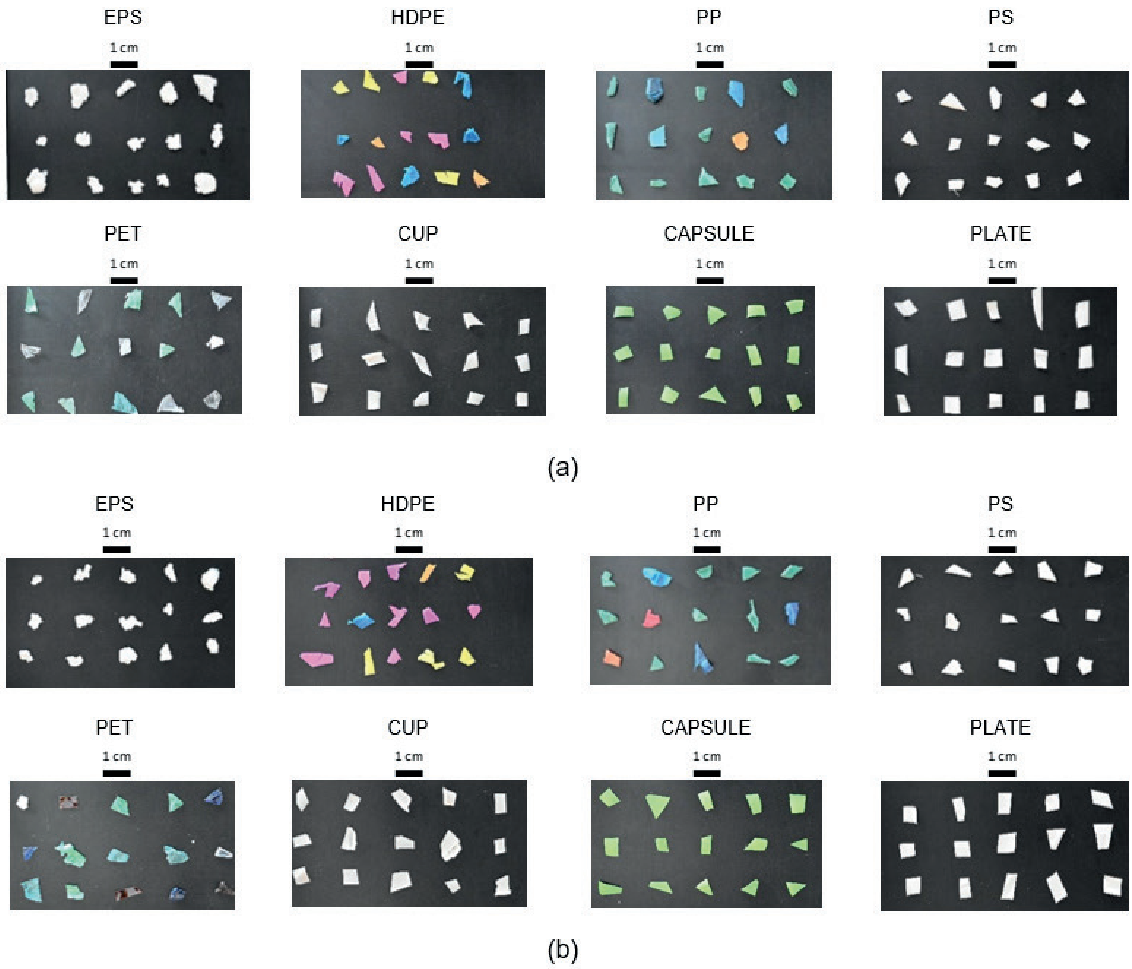

FIGURE 1: Source images of the samples used in this study and their corresponding labels (EPS, PS, PET, HDPE, PP, CUP, CAPSULE, and PLATE): (a) calibration dataset and (b) validation dataset.

able for datasets with many classes and similar spectral signatures, as it organizes the classification into successive levels, progressively separating samples from broad groups to individual classes (Bonifazi et al., 2025). Partial Least Squares - Discriminant Analysis (PLS-DA) was employed as the classification method at each hierarchical level. PLS-DA is a supervised technique that needs prior knowledge of the data (Barker and Rayens, 2003), which is based on the reduction of dimensionality through Partial Least Squares regression (PLS-R) with discriminating characteristics (Ballabio and Todeschini, 2009; Ballabio and Consonni, 2013). An additional class, labelled NC (Not Classified), was included to assign samples that did not meet the acceptance criteria for any predefined class, typically due to exceeding threshold values for Q-residuals or Hotelling's T-squared (T^2) statistic (Eigenvector Research, 2025).

The Venetian Blinds (with a number of data splits equal to 10) cross-validation method was chosen, in order to evaluate the complexity of models and to select the appropriate number of latent variables (LVs) (Eigenvector Research, 2024). Cross-validation was used mainly for model optimization, whereas the predictive capability of the final hierarchical model was assessed using the independent validation dataset.

The classification performances of the model were reported in terms of class predicted member map and statistical parameters in calibration (Cal) and cross-validation (CV) phases: Sensitivity and Specificity (equations 1 and 2).

$$\text{Sensitivity} = \frac{\text{TP}}{\text{TP+FN}} \tag{1}$$

$$\text{Specificity} = \frac{\text{TN}}{\text{TN+FP}} \tag{2}$$

where TN (True Negatives) are correctly identified non-members and FP (False Positives) are samples incorrectly classified as members of the target class. Values approaching 1.0 for both metrics indicate a robust model (Eigenvector Research, 2018).

3. RESULTS AND DISCUSSION

3.1 Average raw and preprocessed reflectance spectra

Figure 2 shows the average raw reflectance spectra and the preprocessed spectra of the analyzed spectral classes. As observed in Figure 2a, the raw spectra exhibit distinct reflectance profiles within the SWIR range (1000-2500 nm),

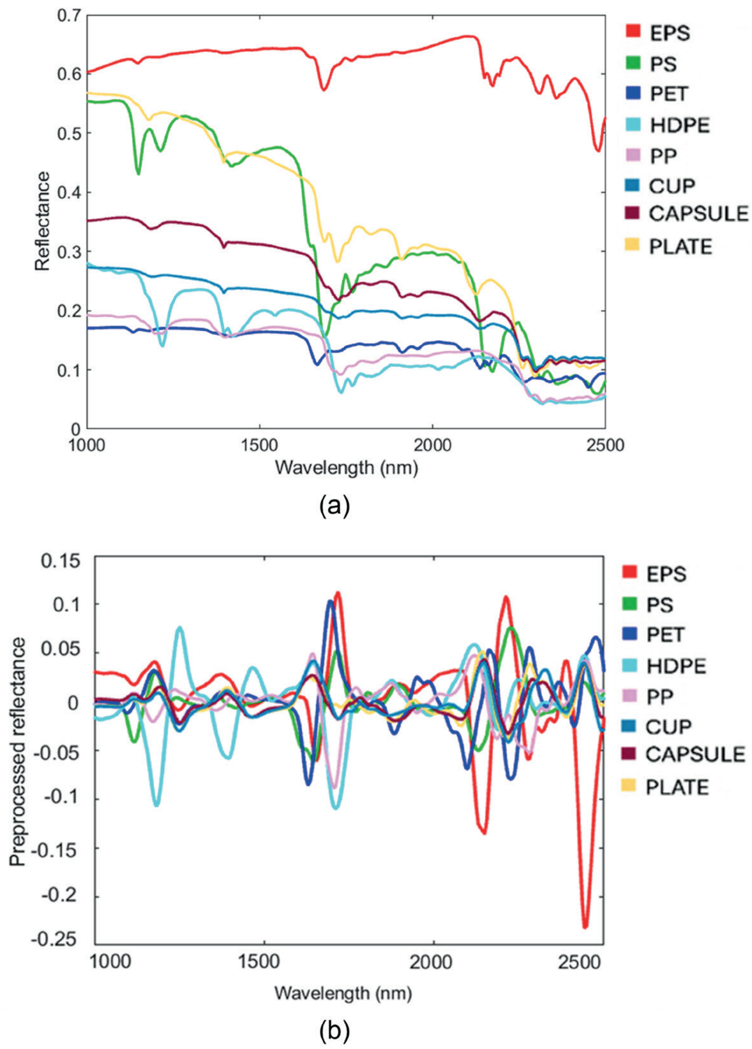

FIGURE 2: (a) Average raw and (b) preprocessed reflectance spectra of the investigated classes in the SWIR range (1000-2500 nm).

which are characteristic of each examined material. In this spectral region, the observed features are mainly related to overtones and combination bands of molecular vibrations involving C–H, O–H and C=O functional groups, which are commonly present in polymeric materials and/or associated additives and residues. In particular, variations in band position, intensity and shape across the investigated classes suggest differences in chemical composition, polymer structure and formulation, supporting the suitability of SWIR spectroscopy for material discrimination. Moreover, as illustrated in Figure 2b, the application of the combined preprocessing strategy (SNV, first derivative with a 5-point window and mean centering), enhanced these spectral differences by reducing scattering effects and emphasizing diagnostic spectral features, thereby improving the characteristic spectral fingerprints of the investigated polymers.

3.2 Hi-PLS-DA model building

The architecture of the hierarchical PLS-DA model (Hi-PLS-DA) was directly supported by the exploratory PCA results obtained after evaluating different preprocessing combinations for each decision rule. As illustrated by the PCA score and loading plots (Figure 3), specific preprocessing strategies enhanced the relevant spectral features and maximized the class separability required at each hierarchical level.

For Rule 1, the combination of SNV, first derivative (11-point window), and mean centering provided a clear separation between fossil-based plastics (EPS, PS, PET, HDPE and PP) and PLA-based bioplastics (CUP, CAPSULE and PLATE), as shown in the PCA score plot (Figure 3a), where PC1 and PC2 explained 51.27% and 22.30% of the total variance, respectively. The corresponding loading plot (Figure 3b) highlighted the spectral variables contributing to the observed class separation. For Rule 2, the same preprocessing strategy of Rule 1 revealed two well-defined spectral macro-groups corresponding to EPS/PS/PET and HDPE/PP, as shown in the PCA score plot (Figure 3c), where PC1 and PC2 explained 53.34% and 23.34% of the total variance, respectively. The corresponding loading plot (Figure 3d) highlighted the spectral variables contributing to the separation between these two macro-groups (EPS/PS/PET and HDPE/PP). For Rule 3, the combination of SNV, first derivative (15-point window), and mean center-

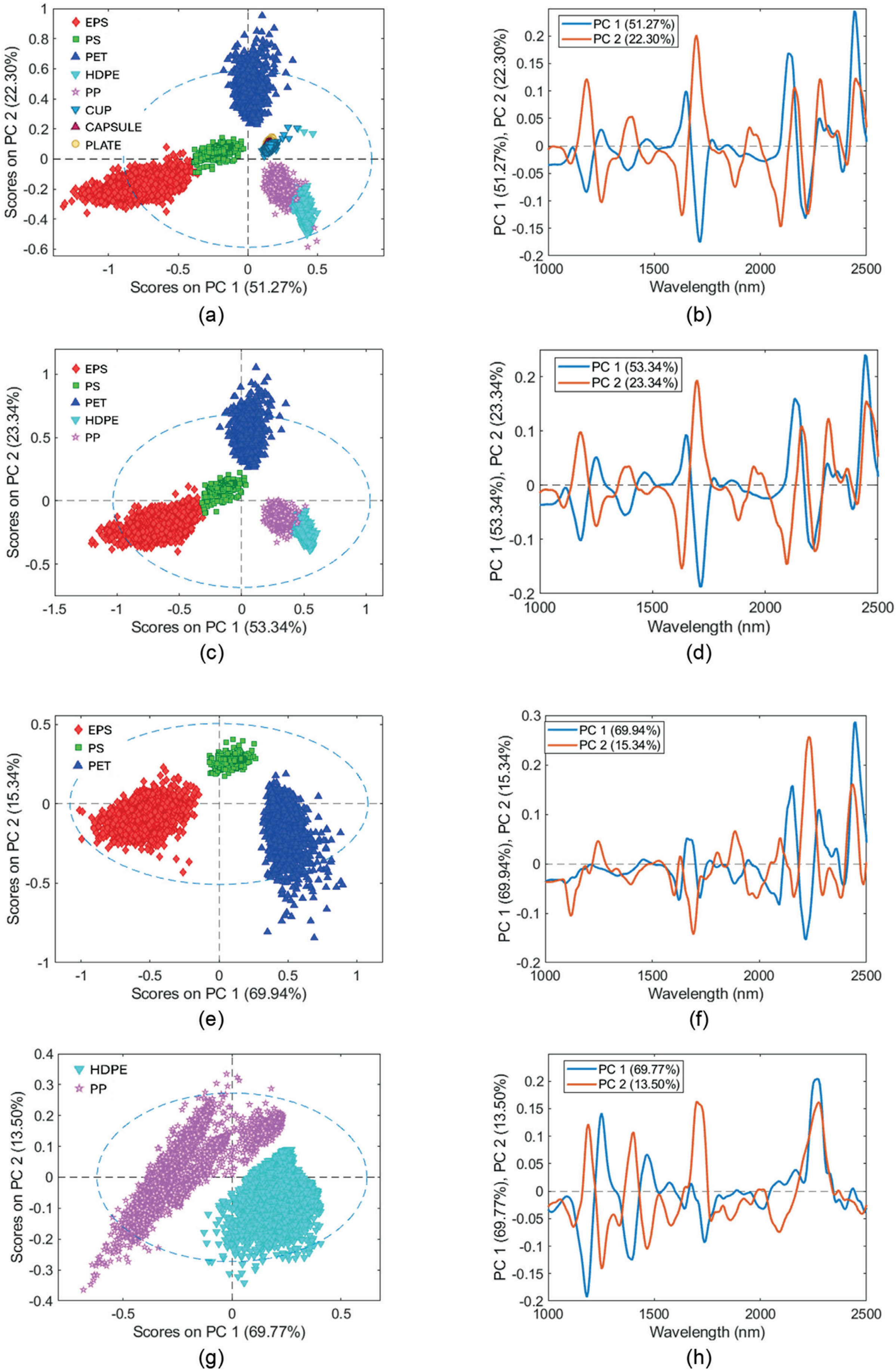
EPS
PS
PET
HDPE
PP
CUP
CAPSULE
PLATE
Scores on PC 1 (51.27%)
Scores on PC 2 (22.30%)
(a)
PC 1 (51.27%)
PC 2 (22.30%)
Wavelength (nm)
PC 1 (51.27%), PC 2 (22.30%)
(b)
EPS
PS
PET
HDPE
PP
Scores on PC 1 (53.34%)
Scores on PC 2 (23.34%)
(c)
PC 1 (53.34%)
PC 2 (23.34%)
Wavelength (nm)
PC 1 (53.34%), PC 2 (23.34%)
(d)
EPS
PS
PET
Scores on PC 1 (69.94%)
Scores on PC 2 (15.34%)
(e)
PC 1 (69.94%)
PC 2 (15.34%)
Wavelength (nm)
PC 1 (69.94%), PC 2 (15.34%)
(f)
HDPE
PP
Scores on PC 1 (69.77%)
Scores on PC 2 (13.50%)
(g)
PC 1 (69.77%)
PC 2 (13.50%)
Wavelength (nm)
PC 1 (69.77%), PC 2 (13.50%)
(h)

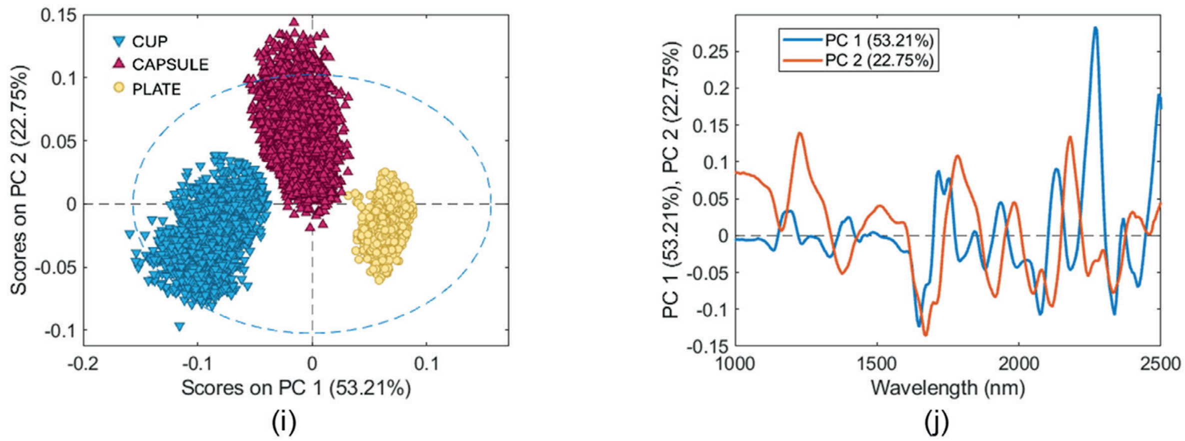

FIGURE 3: Exploratory PCA results obtained after applying the different preprocessing strategies selected for each hierarchical decision rule. (a) PCA score and (b) loading plots of Rule 1; (c) PCA score and (d) loading plots of Rule 2; (e) PCA score and (f) loading plots of Rule 3; (g) PCA score and (h) loading plots of Rule 4; (i) PCA score and (j) loading plots of Rule 5.

ing improved the discrimination among EPS, PS, and PET, as shown in the PCA score plot (Figure 3e), where PC1 and PC2 explained 69.94% and 15.34% of the total variance, respectively. The corresponding loading plot (Figure 3f) highlighted the spectral variables contributing to the discrimination among EPS, PS and PET classes. For Rule 4, the combination of SNV, first derivative (11-point window), and mean centering provided satisfactory separation between polyolefin classes, i.e., HDPE and PP, as shown in the PCA score plot (Figure 3g), where PC1 and PC2 explained 69.77% and 13.50% of the total variance, respectively. The corresponding loading plot (Figure 3h) highlighted the spectral variables contributing to the discrimination between HDPE and PP classes. Finally, for Rule 5, the combination of SNV, Gap Segment first derivative (gap = 5, segment = 5) and mean centering allowed effective discrimination among the three PLA-based bioplastic classes (CUP, CAPSULE and PLATE), as shown in the PCA score plot (Figure 3i), where PC1 and PC2 explained 53.21% and 22.75% of the total variance, respectively. The corresponding loading plot (Figure 3j) highlighted the spectral variables contributing to the discrimination among CUP, CAPSULE and PLATE classes, indicating that, although all samples were PLA-based, differences in formulation, additives, colour and/or product-specific characteristics contributed to their spectral separation.

Overall, the PCA results showed that tailoring the preprocessing to the specific discrimination task at each node improved class separability and provided the rationale for the hierarchical classification model implemented in this study.

Figure 4 shows the resulting hierarchical structure, in which a dedicated PLS-DA model is implemented at each decision node. An optimal number of two LVs was selected for all PLS-DA models. The model architecture was designed to reflect the progressive spectral separability identified during the exploratory analysis using PCA, and it was implemented as a sequence of successive decision rules, i.e., PLS-DA models, from Rule 1 to Rule 5. Samples not fulfilling the classification criteria at any decision level were assigned to the NC (Not Classified) category. The resulting hierarchical structure is detailed as follows:

- Rule 1 was defined in order to provide 3 outputs: (i) fossil-based plastics (EPS, PS, PET, HDPE, PP), which are further classified through Rules 2, 3 and 4; (ii) bioplastics (CUP, CAPSULE and PLATE), which are further classified through Rule 5; (iii) NC.
- Rule 2 was defined in order to provide 3 outputs: (i) EPS, PS and PET, which are further classified through Rule 3; (ii) HDPE and PP, which are further classified through Rule 4; (iii) NC.
- Rule 3 was defined in order to provide 4 outputs: (i) EPS; (ii) PS; (iii) PET; (iv) NC.
- Rule 4 was defined in order to obtain 3 outputs: (i) HDPE; (ii) PP; (iii) NC.
- Rule 5 was defined in order to obtain 4 outputs: (i) CUP; (ii) CAPSULE; (iii) PLATE; (iv) NC.

3.3 Classification results

The class-predicted hyperspectral maps obtained using the Hi-PLS-DA model showed strong agreement with the expected polymer classes in the validation dataset (Figure 5). The model correctly discriminated fossil-based plastics and bioplastic samples, preserving their spatial distribution within the hyperspectral image. Comparison with the ground truth (Figure 5a), thus, confirmed the reliability of the classification, with misclassifications limited to a small number of pixels located mainly along sample edges (Figure 5b). In some cases, these discrepancies can be attributed to light-scattering effects and border effects at sample edges, which can lead to spectral mixing and alter the recorded reflectance signal at the pixel level. This behavior is commonly observed in pixel-wise hyperspectral classification, where boundary pixels may include mixed spectral information from the target material and the surrounding background or adjacent regions.

The statistical results reported in Table 1 confirm the high performance and stability of the hierarchical Hi-PLS-DA model across all decision rules, with very consistent values between calibration (Cal) and cross-validation (CV)

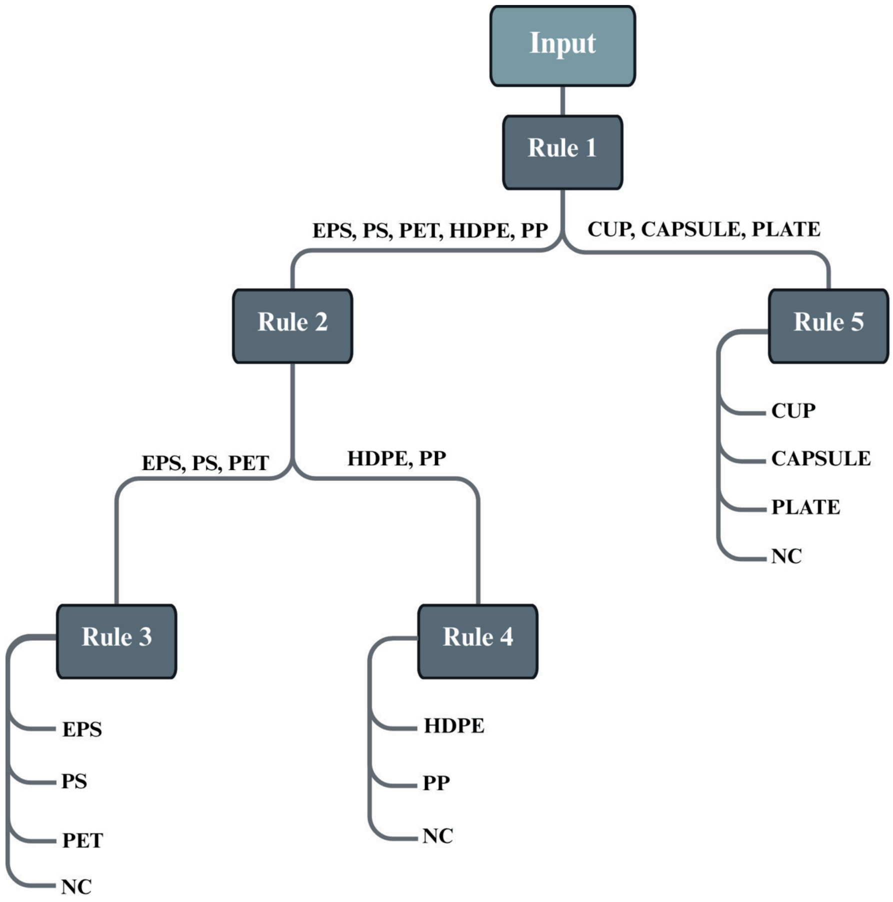

FIGURE 4: Hierarchical structure of the Hi-PLS-DA classification model, showing the five sequential decision rules. NC = Not Classified.

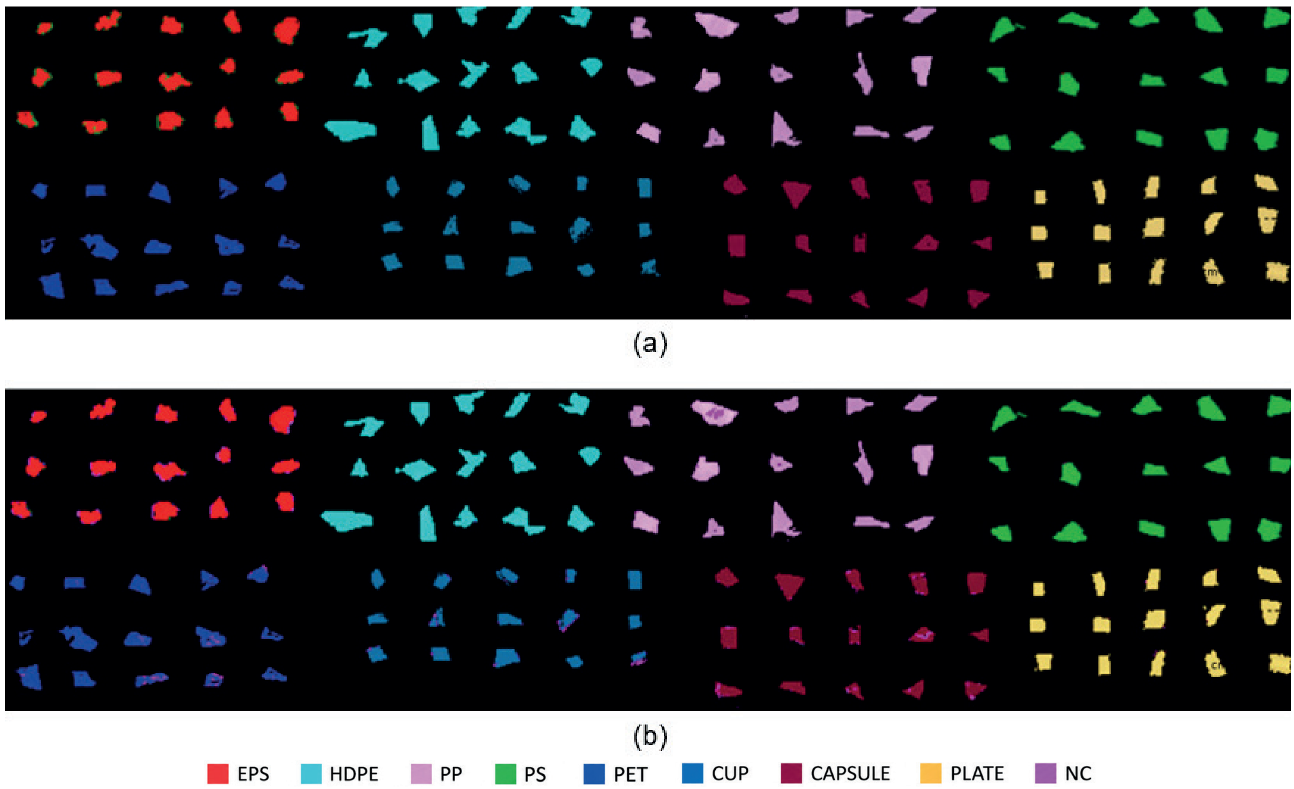

FIGURE 5: Validation dataset with (a) the expected classes and (b) the predicted classes obtained by Hi-PLS-DA. NC = Not Classified.

TABLE 1: Statistical parameters of calibration dataset from Rule 1 to Rule 5, in calibration (Cal) and cross-validation (CV) phases.

Rules	Classes	Sensitivity (Cal)	Specificity (Cal)	Sensitivity (CV)	Specificity (CV)
RULE 1	EPS/PS/PET/HDPE/PP	0.99	0.99	0.99	0.99
	CUP/CAPSULE/PLATE	0.99	0.99	0.99	0.99
RULE 2	EPS/PS/PET	1.00	1.00	1.00	1.00
	HDPE/PP	1.00	1.00	1.00	1.00
RULE 3	EPS	0.99	0.99	0.99	0.99
	PS	0.98	0.99	0.98	0.99
	PET	1.00	0.99	1.00	0.99
RULE 4	HDPE	0.99	0.99	0.99	0.99
	PP	0.99	0.99	0.99	0.99
RULE 5	CUP	0.99	0.97	0.99	0.97
	CAPSULE	0.98	0.98	0.98	0.98
	PLATE	0.99	0.99	0.99	0.99

phases. The results achieved for each rule are reported in the following.

Rule 1 provided high discrimination between PLA-based bioplastics and fossil-based plastics, with sensitivity and specificity values of 0.99 in both Cal and CV. Rule 2 achieved perfect classification (sensitivity and specificity = 1.00 in Cal and CV) for the discrimination between the two fossil-based macro-groups (HDPE/PP vs PS/EPS/PET). Rule 3, focused on the discrimination among EPS, PS, and PET, also showed very high performance, with sensitivity and specificity values from 0.98 to 1.00 in Cal and CV. Rule 4 achieved sensitivity and specificity values of 0.99 in both Cal and CV for the discrimination between HDPE and PP. Rule 5, related to the classification of PLA-based bioplastics (CUP, CAPSULE and PLATE), also exhibited high performance in Cal and CV, with sensitivity values between 0.98 and 0.99 and specificity between 0.97 and 0.99.

The prediction results obtained on the independent validation dataset (Table 2) further confirmed the robustness and generalization capability of the proposed Hi-PLS-DA model. Sensitivity values ranged from 0.96 to 1.00, while specificity values varied between 0.99 and 1.00. PET achieved perfect sensitivity (1.00), whereas PS showed the lowest sensitivity (0.96), although maintaining a specificity of 0.99. The remaining polymer classes exhibited sensitivity and specificity values equal to or higher than 0.98 and 0.99, respectively, demonstrating the excellent predictive performance of the proposed hierarchical classification strategy.

TABLE 2: Statistical parameters of validation dataset in prediction (Pred) phase.

Classes	Sensitivity (Pred)	Specificity (Pred)
EPS	0.99	0.99
PS	0.96	0.99
PET	1.00	0.99
HDPE	0.98	0.99
PP	0.99	0.99
CUP	0.99	1.00
CAPSULE	0.99	0.99
PLATE	0.99	0.99

Overall, the prediction results confirmed the capability of the proposed hierarchical Hi-PLS-DA model to accurately discriminate both fossil-based plastics and PLA-based bioplastics, as demonstrated by the predicted hyperspectral maps of the independent validation dataset and the corresponding statistical parameters.

4. CONCLUSIONS

This study demonstrated the feasibility of combining SWIR-HSI (1000-2500 nm), PCA-guided preprocessing optimization, and Hi-PLS-DA model for the discrimination of fossil-based plastics and PLA-based bioplastics in plastic waste flakes. The hierarchical classification strategy, designed according to the progressive spectral separability identified by PCA, enabled accurate polymer discrimination while maintaining high classification performance throughout the hierarchical decision process.

Although conceived as a proof of concept, the proposed methodology addresses an emerging challenge associated with the increasing diffusion of bioplastics in conventional plastic recycling streams. Reliable identification of these materials is becoming increasingly important to prevent contamination of fossil-based plastic recycling streams and preserve the quality of secondary raw materials from plastic packaging waste. In this context, the proposed workflow represents a promising methodological basis for the future development of optical sensor-based sorting strategies capable of managing increasingly heterogeneous plastic waste streams. This study focused on PLA-based bioplastic packaging products and did not cover the full range of commercially available biopolymers. Nevertheless, the high discrimination capability achieved among compositionally related PLA-based samples demonstrates the sensitivity of SWIR-HSI to subtle spectral differences associated with formulation, additives, and product-specific characteristics. These results provide a sound basis for extending the proposed approach to a broader range of commercially available biopolymers in future recycling-oriented sorting applications. Furthermore, this evidence suggests that SWIR-HSI, especially when combined with multivariate and hierarchical classification strategies, may represent a promising tool for extending the identification of biopolymer-based materials in recycling-oriented sorting applications.

Future work will focus on expanding the spectral library to include a wider range of commercial fossil-based polymers and bioplastic formulations, colors, additives, fillers, ageing conditions, surface contamination and real post-consumer materials. The evaluation of the proposed methodology under representative industrial sorting conditions will also be essential to assess its robustness and practical applicability, supporting the production of high-quality secondary raw materials by reducing cross-contamination between conventional plastics and PLA-based bioplastics during optical sorting.

REFERENCES

Alaerts, L., Augustinus, M., & Van Acker, K. (2018). Impact of bio-based plastics on current recycling of plastics. Sustainability (Switzerland), 10(5). https://doi.org/10.3390/su10051487

Araujo-Andrade, C., Bugnicourt, E., Philippet, L., Rodriguez-Turienzo, L., Nettleton, D., Hoffmann, L., & Schlummer, M. (2021). Review on the photonic techniques suitable for automatic monitoring of the composition of multi-materials wastes in view of their posterior recycling. Waste management & research, 39(5), 631-651.

Ballabio, D., and Todeschini, R., (2009). Multivariate classification for qualitative analysis, New York In D.-W. Sun (Ed.). Infrared spectroscopy for quality analysis and control, 83–104.

Ballabio, D. and Consonni, V., (2013). Classification tools in chemistry. Part 1: Linear models. PLS-DA, Analytical Methods, 5, 3790-3798.

Barker, M., Rayens, W., (2003). Partial least squares for discrimination. Journal of Chemometrics, 17 (3), 166–173. https://doi.org/10.1002/cem.785

Bonifazi, G., Capobianco, G., Cucuzza, P., Serranti, S., & Uzzo, A. (2022). Recycling-oriented characterization of the PET waste stream by SWIR hyperspectral imaging and variable selection methods. Detritus, 18, 42-49.

Bonifazi, G., Capobianco, G., Cucuzza, P., & Serranti, S. (2025a). Contaminant detection in flexible polypropylene packaging waste using hyperspectral imaging and machine learning. Waste Management, 195, 264-274.

Bonifazi, G., Capobianco, G., Cucuzza, P., & Serranti, S. (2025b, May). Application of hyperspectral imaging for identifying polymer blends in polypropylene flexible packaging waste for enhanced recycling. In Algorithms, Technologies, and Applications for Multispectral and Hyperspectral Imaging XXXI (Vol. 13455, pp. 266-274). SPIE.

Bro, R., Smilde, A.K., (2014). Principal component analysis. Analytical Methods, 6, 2812. https://doi.org/10.1039/c3ay41907j

Cheng, M. F., Mukundan, A., Karmakar, R., Valappil, M. A. E., Jouhar, J., & Wang, H. C. (2025). Modern trends and recent applications of hyperspectral imaging: A review. Technologies, 13(5), 170.

Cosate de Andrade, M. F., Souza, P. M., Cavalett, O., & Morales, A. R. (2016). Life cycle assessment of poly (lactic acid)(PLA): Comparison between chemical recycling, mechanical recycling and composting. Journal of Polymers and the Environment, 24(4), 372-384.

Das, A., Mishra, S., Tripathy, B. (2025). Bioplastics: a sustainable alternative or a hidden microplastic threat?. Innovative Infrastructure Solutions. 10(7), 321.

Cucina, M., De Nisi, P., Trombino, L., Tambone, F., & Adani, F. (2021). Degradation of bioplastics in organic waste by mesophilic anaerobic digestion, composting and soil incubation. Waste Management, 134, 67-77.

De Gisi, S., Gadaleta, G., Gorrasi, G., La Mantia, F. P., Notarnicola, M., & Sorrentino, A. (2022). The role of (bio) degradability on the management of petrochemical and bio-based plastic waste. Journal of Environmental Management, 310, 114769.

Eigenvector Research, 2011. Mncn. https://www.eigenvectordocs.com/index.php?title=Mncn (accessed on 01 May 2026).

Eigenvector Research, 2013. Gapsegment. https://www.eigenvectordocs.com/index.php?title=Gapsegment#Purpose (accessed on 01 May 2026)

Eigenvector Research, 2018. Confusionmatrix. https://www.eigenvectordocs.com/index.php?title=Confusionmatrix (accessed on 01 May 2026).

Eigenvector Research, 2019. Advanced Preprocessing: Noise, Offset, and Baseline Filtering. https://www.eigenvectordocs.com/index.php?title=Advanced_Preprocessing:_Noise,_Offset,_and_Baseline_Filtering#Detrend (last accessed on 01 May 2026).

Eigenvector Research, 2021. Advanced Preprocessing: Sample Normalization. https://www.eigenvectordocs.com/index.php?title=Advanced_Preprocessing:_Sample_Normalization (accessed on 01 May 2026).

Eigenvector Research, 2024. Crossval. https://www.eigenvectordocs.com/index.php?title=Crossval (accessed on 01 May 2026).

Eigenvector Research, 2025. T-Squared Q residuals and Contributions. https://www.eigenvectordocs.com/index.php?title=T-Squared_Q_residuals_and_Contributions (accessed on 01 May 2026).

European Bioplastics, 2025. Article 9 PPWR – Why certain packaging formats should be compostable. https://www.european-bioplastics.org/article-9-ppwr-why-certain-packaging-formats-should-be-compostable/ (accessed on 02 May 2026).

European Commission, 2024. Packaging and packaging waste regulation (PPWR). https://environment.ec.europa.eu/document/download/63fd2c88-e85a-412c-bcf4-372eff99008a_en (accessed on 02 May 2026).

Gadaleta, G., Ferrara, C., De Gisi, S., Notarnicola, M., & De Feo, G. (2023). Life cycle assessment of end-of-life options for cellulose-based bioplastics when introduced into a municipal solid waste management system. Science of the Total Environment, 871, 161958.

Lavagnolo, M.C., Ruggero, F., Pivato, A., Boaretti, C., Chiumenti, A. (2020). Composting of starch-based bioplastic bags: small scale test of degradation and size reduction trend. Detritus. 57–65.

Li, M., Cai, Q., Zhang, T., Tang, H., & Li, H. (2025). Progress of complex system process analysis based on modern spectroscopy combined with chemometrics. Journal of Chemometrics, 39(2), e70006.

McLauchlin, A. R., Ghita, O., & Gahkani, A. (2014). Quantification of PLA contamination in PET during injection moulding by in-line NIR spectroscopy. Polymer Testing, 38, 46-52.

Pottinger, A. S., Geyer, R., Biyani, N., Martinez, C. C., Nathan, N., Morse, M. R., Shanying Hu, C. L., de Bruyn, M., Boettiger, C., Baker, E., & McCauley, D. J. (2024). Pathways to reduce global plastic waste mismanagement and greenhouse gas emissions by 2050. Science, 386(6726), 1168-1173.

Rinnan, Å., van den Berg, F.M., Engelsen, S.B., 2009. Review of the most common pre-processing techniques for near-infrared spectra, TrAC Trends Anal. Chem, 28, pp. 1201-1222.

Serranti, S., Cucuzza, P., & Bonifazi, G. (2020, November). Hyperspectral imaging for VIS-SWIR classification of post-consumer plastic packaging products by polymer and color. In SPIE Future Sensing Technologies (Vol. 11525, pp. 212-217). SPIE.

Serranti, S., Bonifazi, G., Cocozza, P., Cucuzza, P., Palmieri, R., Benzi, M., Lezzi M., Mazziotti C., Riccardi E., Barbieri E., Ingrando I., & Moroni, F. (2026). Comparison of hyperspectral imaging and FTIR spectroscopy for microplastic polymer identification: Proposal of a scalable protocol validated in a 12-month river survey. Talanta, 129361.

Taneepanichskul, N., Hailes, H. C., & Miodownik, M. (2025). Using hyperspectral imaging and machine learning to identify food-contaminated compostable and recyclable plastics. UCL Open Environment, 7. https://doi.org/10.14324/111.444/ucloe.3237

Ulrici, A., Serranti, S., Ferrari, C., Cesare, D., Foca, G., & Bonifazi, G. (2013). Efficient chemometric strategies for PET–PLA discrimination in recycling plants using hyperspectral imaging. Chemometrics and Intelligent Laboratory Systems, 122, 31-39.

Vidal, M., Amigo, J.M., (2012). Pre-processing of hyperspectral images. Essential steps before image analysis. Chemometrics and Intelligent Laboratory Systems, 117, pp. 138-148. https://doi.org/10.1016/j.chemolab.2012.05.009